



# 1 Morphologic and Morphometric Differences between Gullies Formed 2 in Different Substrates on Mars: New Insights into the Gully 3 Formation Processes

4 Rishitosh K. Sinha<sup>1,2</sup>, Dwijesh Ray<sup>1</sup>, Tjalling De Haas<sup>3</sup>, Susan J. Conway<sup>4</sup>, Axel Noblet<sup>4</sup>

5 <sup>1</sup> Physical Research Laboratory, Ahmedabad 380009, Gujarat, India

6 <sup>2</sup> Indian Institute of Technology, Gandhinagar 382355, Gujarat, India

7 <sup>3</sup> Faculty of Geoscience, Universiteit Utrecht, Princetonlaan 8a, 3584 CB Utrecht, the Netherlands

8 <sup>4</sup> Nantes Université, Université d'Angers, Le Mans Université, CNRS UMR 6112 Laboratoire de Planétologie et Géosciences,  
9 France

10

11 *Correspondence to:* Rishitosh K. Sinha (rishitosh@prl.res.in)

12 **Abstract.** Martian gullies are kilometer-scale geologically young features with a source alcove, transportation channel, and  
13 depositional fan. On the walls of impact craters, these gullies typically incise into bedrock or surfaces modified by latitude  
14 dependent mantle (LDM; inferred as consisting ice and admixed dust) and glaciation. To better understand the differences in  
15 alcoves and fans of gullies formed in different substrates and infer the flow types that led to their formation, we have analyzed  
16 the morphology and morphometry of 167 gully systems in 29 craters distributed between 30°S and 75°S. Specifically we  
17 measured length, width, gradient, area, relief, and relief ratio of alcove and fan, melton ratio, relative concavity index, and  
18 perimeter, form factor, elongation ratio and circularity ratio of the alcoves. Our study reveals that alcoves formed in  
19 LDM/glacial deposits are more elongated than the alcoves formed in bedrock, and possess a distinctive V-shaped cross section.  
20 We have found that mean gradient of fans formed by gullies sourced in bedrock is steeper than the mean gradient of fans of  
21 gullies sourced in LDM/glacial deposits. These differences between gullies were found to be statistically significant and  
22 discriminant analysis has confirmed that alcove perimeter, alcove relief and fan gradient are the most important variables for  
23 differentiating gullies according to their source substrates. The comparison between the melton ratio, alcove length and fan  
24 gradient of Martian and terrestrial gullies reveals that Martian gully systems were likely formed by terrestrial debris-flow like  
25 processes. It is likely that the present-day sublimation of CO<sub>2</sub> ice on Mars provided the adequate flow fluidization for the  
26 formation of deposits akin to terrestrial debris-flow like deposits.

## 27 1 Introduction

28 Gullies are found on steep slopes polewards of about 30° latitude in both hemispheres on Mars and manifest as kilometer-  
29 scale, geologically young features (formed within the last few million years) comprising an alcove, channel, and depositional  
30 fan (Malin and Edgett, 2000; Dickson et al., 2007; Reiss et al., 2004; Schon et al., 2009). Gullies occur in a wide assortment



31 of settings, varying from the walls and central peaks of craters to walls of valleys, and steep faces of dunes, hills and polar pits  
32 (e.g. Balme et al., 2006; Dickson et al., 2007; Dickson and Head, 2009; Conway et al., 2011, 2015; Harrison et al., 2015). On  
33 the walls of craters, gullies are found to have incised into the (1) surfaces covered by latitude dependent mantle (LDM; e.g.  
34 Mustard et al., 2001; Dickson et al., 2012, 2015), (2) surfaces modified by former episodes of glaciation (Hubbard et al., 2011;  
35 Souness et al., 2012; Souness and Hubbard, 2012; Sinha and Vijayan, 2017), and (3) bedrock (e.g. Johnsson et al., 2014; de  
36 Haas et al., 2019a; Sinha et al., 2020). Detailed investigation of the gullies formed over these different substrates is key to  
37 understanding the intricacies of past processes by which these gullies have formed on Mars (Conway et al., 2015; de Haas et  
38 al., 2019a).

39 A variety of models have been proposed to explain the formation of gullies, which include: (1) dry flows triggered by  
40 sublimation of CO<sub>2</sub> frost (e.g. Cedillo-Flores et al., 2011; Dundas et al., 2012, 2015; Pilorget and Forget, 2016; de Haas et al.,  
41 2019b), (2) debris-flows of an aqueous nature (e.g. Costard et al., 2002; Levy et al., 2010; Conway et al., 2011; Johnsson et  
42 al., 2014; de Haas et al., 2019a; Sinha et al., 2020), and (3) fluvial flows (e.g. Heldmann and Mellon, 2004; Heldmann et al.,  
43 2005; Dickson et al., 2007; Reiss et al., 2011). To better understand the gully formation processes, morphometric investigation  
44 of gullies formed over different substrates needs to be undertaken at a level of detail previously not attempted.

45 The global distribution of gullies shows a spatial correlation with the landforms indicative of glaciation and LDM deposition  
46 on Mars (e.g. Levy et al., 2011; Dickson et al., 2015; Harrison et al., 2015; Conway et al., 2018; de Haas et al., 2019a; Sinha  
47 et al., 2020). With respect to glacial landforms, many gullies have formed into viscous flow features (VFF) and they are found  
48 in the same extent of latitudes (e.g. Arfstrom and Hartmann, 2005; de Haas et al., 2018). VFFs cover a broad range of landforms  
49 that include lobate debris aprons, concentric crater fill, and lineated valley fills (e.g. Squyres, 1978; Levy et al., 2009; Baker  
50 et al., 2010). Together, they are inferred to be similar to terrestrial debris-covered glaciers (Conway et al., 2018). With respect  
51 to LDM, gullies are mostly found on the pole-facing slopes of crater walls at lower mid-latitudes (30-45°) (e.g. Balme et al.  
52 2006; Kneissl et al. 2010; Harrison et al. 2015; Conway et al. 2017), wherein, LDM is found to be dissected (e.g. Mustard et  
53 al., 2001; Milliken et al., 2003; Head et al., 2003). In the higher latitudes (>45°), LDM is found to be continuous (e.g.  
54 Kreslavsky and Head, 2000), and gullies are evident at both the pole and equator facing slopes (e.g. Balme et al. 2006; Kneissl  
55 et al. 2010; Harrison et al. 2015; Conway et al. 2017). Gullies formed on the formerly glaciated walls of craters are fed from  
56 alcoves that do not extend up to the crater rim, and appear elongated to V-shaped, implying gully-channel incision into ice-  
57 rich, unlithified sediments (e.g. Aston et al., 2011; de Haas et al., 2019a). The alcoves, channels and fan deposits of gullies  
58 formed within craters covered by a smooth drape of LDM, are usually found to have experienced multiple episodes of LDM  
59 covering and subsequent reactivation of some of the pre-existing channels or formation of fresh channels within the draped  
60 LDM deposits (e.g. Dickson et al., 2015; de Haas et al., 2019a). Additionally, there are gullies that directly emanate from well-  
61 defined bedrock alcoves that cut into the crater rim in the absence of LDM and/or glacial deposits (e.g. Johnsson et al., 2014;  
62 de Haas et al., 2019a; Sinha et al., 2020). Gullies formed in these craters have alcoves with sharply defined crests and spurs,



63 exposing the underlying bedrock, and meter-sized boulders are found throughout the gully system (e.g. Johnsson et al., 2014;  
64 de Haas et al., 2019a; Sinha et al., 2020). Further, De Haas et al., 2015a found that the stratigraphy of the fans whose source  
65 area was in bedrock were more boulder-rich than those fans fed by catchments in LDM. The findings in these studies suggest  
66 that a more detailed investigation of the morphology and morphometry of the gullies formed over contrasting substrates is  
67 important for improving our understanding of the formative mechanisms of gullies.

68 In this work, we focus on addressing the following research questions:

69 (1) Do the morphology and morphometry of gully systems formed in different substrates differ (i.e. LDM/glacial deposits and  
70 bedrock)?

71 (2) How do the morphometric characteristics of gullies formed on Mars compare to those formed by a range of processes on  
72 Earth, and what does that tell us about the formative processes of Martian gullies?

73 To parameterize the morphometry we will primarily study long profiles. Previously, only a few studies have analyzed the  
74 morphometric characteristics of the gullies by studying long profiles of gullies (e.g. Yue et al., 2014; Conway et al., 2015; De  
75 Haas et al., 2015a; Hobbs et al., 2015). These studies have focused observations on a part of the gully system and suggested  
76 that the differences in the properties of substrate into which the gullies incise play a significant role in promoting the flows  
77 that led to gully formation. Hence, for a more detailed differentiation of the gully types and interpretation of the dominant flow  
78 type that led to gully formation on Mars, quantification of the morphometric characteristics of the entire gully system is crucial.

## 79 **2 Study sites and datasets**

80 We characterize the morphology and morphometry of gullies in 29 craters distributed over the southern hemisphere between  
81 30° S and 75° S latitude (Fig. 1). These 29 craters are selected based on the availability of publicly released High Resolution  
82 Imaging Science Experiment (HiRISE) stereo-pair based digital terrain model (DTM) or the presence of suitable HiRISE  
83 stereo-pair images to produce a DTM ourselves. The HiRISE stereo-pair images are usually ~0.25 - 0.5 m/pixel (McEwen et  
84 al., 2007), so the DTM post spacing is ~1-2 m with vertical precision in the range of tens of centimeters (Kirk et al., 2008).  
85 Among the 29 gullied craters, publicly released DTMs are available for 25 craters  
86 (<https://www.uahirise.org/hiwish/maps/dtms.jsp> - last accessed 18th September 2021) (Table 1). For the remaining 4 craters,  
87 DTMs are produced with the software packages USGS ISIS and BAE Systems SocetSet (Table 1) (Kirk et al., 2008). We  
88 investigated HiRISE images of these 29 gullied craters for detailed morphological characterization of the substrate into which  
89 the crater wall gullies incise (Table 1).

90

91



92 **Table 1.** Summary of the craters included in this study, their locations, diameter, substrate on the crater wall in which gullies  
 93 have incised, key morphological attributes of the substrate, and IDs of HiRISE imagery and DTM used for morphological and  
 94 morphometric investigation of gullies in these craters.

Crater	Latitude	Longitude	Substrate	Key morphological attributes	HiRISE ID	HiRISE DTM ID
Artik	34.8° S	131.02° E	LDM/glacial deposits	Polygons, V-shaped incisions, arcuate ridges, small-scale LDAs on the floor	ESP_020740_1450	DTEEC_012459_1450_01 2314_1450_A01
Asimov	47.53° S	4.41° E	LDM/glacial deposits	Polygons, V-shaped incisions, mantled alcoves/channels/fans, arcuate ridges, small-scale LDAs inside valleys	ESP_012912_1320	DTEEC_012912_1320_01 2767_1320_A01
Bunnik	38.07° S	142.07° W	LDM/glacial deposits	Polygons, V-shaped incisions, mantled alcoves/channels/fans, arcuate ridges	ESP_047044_1420	DTEEC_002659_1420_00 2514_1420_U01
Corozal	38.78° S	159.48° E	LDM/glacial deposits	Polygons, mantled alcoves/channels/fans, arcuate ridges, small-scale LDAs on the floor	PSP_006261_1410	DTEEC_006261_1410_01 4093_1410_A01
Dechu	42.23° S	158° W	LDM/glacial deposits	Polygons, mantled alcoves/channels/fans, arcuate ridges, small-scale LDAs on the floor	PSP_006866_1375	DTEED_023546_1375_02 3612_1375_A01
Dunkassa	37.46° S	137.06° W	LDM/glacial deposits	Polygons, V-shaped incisions, mantled alcoves/channels/fans, arcuate ridges, small-scale LDAs on the floor	ESP_032011_1425	DTEEC_039488_1420_03 9343_1420_A01
Hale	35.7° S	36.4° W	LDM/glacial deposits	Polygons, V-shaped incisions, mantled alcoves/channels/fans, talus slope deposits	PSP_003209_1445	DTEEC_002932_1445_00 3209_1445_A01
Langtang	38.13° S	135.95° W	LDM/glacial deposits	Polygons, V-shaped incisions, mantled alcoves/channels/fans, arcuate ridges, small-scale LDAs on the floor	ESP_030099_1415	DTEEC_024099_1415_02 3809_1415_U01



Moni	46.97° S	18.79° E	LDM/glacial deposits	Partly infilled alcoves, mantled fan surfaces, arcuate ridges	ESP_056862_1325	DTEEC_007110_1325_006820_1325_A01
Nybyen	37.03° S	16.66° W	LDM/glacial deposits	Polygons, mantled alcoves/channels/fans, arcuate ridges	ESP_059448_1425	DTEEC_006663_1425_011436_1425_A01
Palikir	41.56° S	157.87° W	LDM/glacial deposits	Polygons, V-shaped incisions, mantled alcoves/channels/fans, arcuate ridges, small-scale LDAs on the floor	ESP_057462_1380	DTEEC_005943_1380_011428_1380_A01
Penticton	38.38° S	96.8° E	LDM/glacial deposits	Polygons, V-shaped incisions, mantled alcoves/channels/fans, arcuate ridges, small-scale LDAs on the floor	ESP_029062_1415	DTEEC_001714_1415_001846_1415_U01
Selevac	37.37° S	131.07° W	LDM/glacial deposits	Polygons, mantled alcoves/channels/fans, small-scale flows on the floor	ESP_045158_1425	DTEEC_003252_1425_003674_1425_A01
Raga	48.1° S	117.57° W	LDM	Polygons, mantled alcoves/channels/fans	ESP_041017_1315	DTEEC_014011_1315_014288_1315_A01
Roseau	41.7° S	150.6° E	LDM	Polygons, mantled alcoves/channels/fans	ESP_024115_1380 / ESP_011509_1380	ESP_024115_1380_ESP_011509_1380*
Taltal	39.5° S	125.8° W	LDM/glacial deposits	Polygons, V-shaped incisions, mantled alcoves/channels/fans, arcuate ridges, small-scale LDAs on the floor	ESP_037074_1400 / ESP_031259_1400	ESP_037074_1400_ESP_031259_1400*
Talu	40.34° S	20.11° E	LDM/glacial deposits	Polygons, V-shaped incisions, mantled alcoves/channels/fans, arcuate ridges, small-scale LDAs on the floor	ESP_011817_1395	DTEEC_011817_1395_011672_1395_O01
Triolet	37.08° S	168.02° W	LDM/glacial deposits	Polygons, V-shaped incisions, mantled alcoves/channels/fans, arcuate ridges, small-scale LDAs on the floor	ESP_047190_1425	DTEEC_023586_1425_024008_1425_A01
Unnamed crater	32.31° S	118.55° E	LDM/glacial deposits	Polygons, mantled alcoves/channels/fans, arcuate ridges, small-	PSP_006869_1475	DTEEC_021914_1475_022336_1475_U01



				scale LDAs on the floor		
Unnamed crater in the Argyre basin	40.3° S	40.4° W	LDM/glacial deposits	Polygons, mantled alcoves/channels/fans, arcuate ridges, small-scale LDAs on the floor	ESP_032047_1395	DTEEC_012795_1395_013507_1395_A01
Unnamed crater in the Newton basin	38.8° S	156.8° W	LDM	Polygons, V-shaped incisions, mantled alcoves/channels/fans	PSP_002686_1410	DTEEC_002620_1410_002686_1410_A01
Unnamed crater north of Corozal crater	38.53° S	159.44° E	LDM/glacial deposits	Polygons, mantled alcoves/channels/fans, small-scale LDAs on the floor	ESP_020884_1410	DTEEC_020884_1410_020950_1410_A01
Unnamed crater-1 in the Terra Sirenum	32.55° S	154.11° W	LDM	Mantled alcoves/channels/fans	PSP_007380_1470	DTEEC_010597_1470_007380_1470_U01
Unnamed crater-2 in the Terra Sirenum	38.88° S	136.36° W	LDM/glacial deposits	Polygons, V-shaped incisions, mantled alcoves/channels/fans, arcuate ridges, small-scale LDAs on the floor	ESP_020407_1410	DTEEC_022108_1410_022385_1410_A01
Istok	45.1° S	85.82° W	Bedrock	Alcove cut directly into the original crater-wall material, clasts embedded into fresh deposits on fan	ESP_056668_1345	DTEEC_040607_1345_040251_1345_A01
Galap	37.66° S	167.07° W	Bedrock	Alcove cut directly into the original crater-wall material, clasts embedded into fresh deposits on fan	ESP_059770_1420	DTEEC_048983_1420_048693_1420_U01
Gasa	35.73° S	129.4° E	Bedrock	Alcove cut directly into the original crater-wall material, clasts embedded into fresh deposits on fan	ESP_057491_1440	DTEEC_021584_1440_022217_1440_A01
Los	35.08° S	76.23° W	Bedrock	Alcove cut directly into the original crater-wall material, clasts embedded into fresh deposits on fan	ESP_020774_1445 / ESP_050127_1445	ESP_020774_1445_ESP_050127_1445*

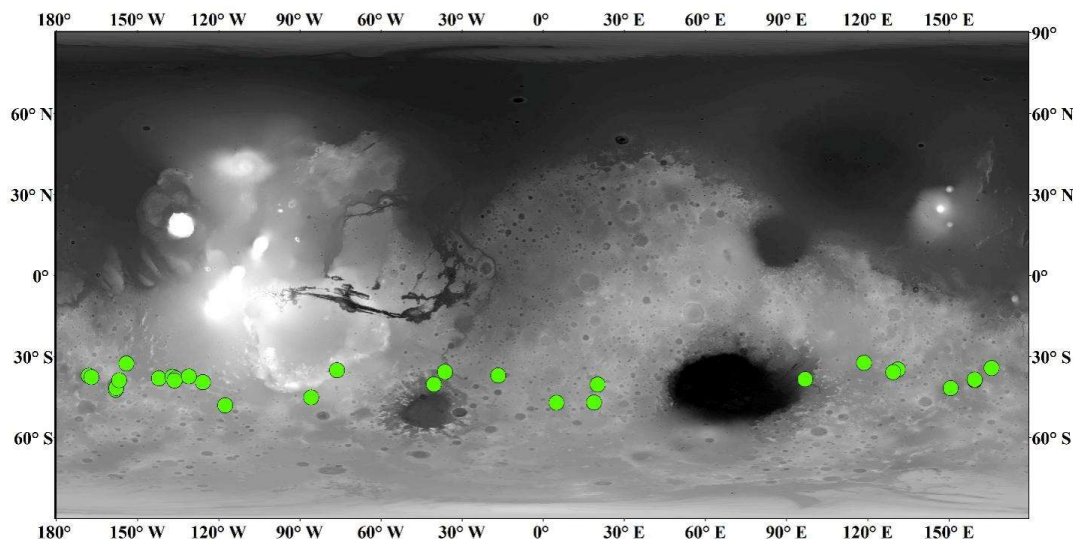


Unnamed crater-3 in the Terra Sirenum	34.27° S	165.71° E	Bedrock	Alcove cut directly into the original crater-wall material, clasts embedded into fresh deposits on fan	ESP_049261_1455 / ESP_049828_1455	ESP_049261_1455_ ESP_049828_1455*
---------------------------------------	----------	-----------	---------	--	-----------------------------------	-----------------------------------

95

96 (\*) DTMs are produced with the software packages USGS ISIS and BAE Systems SocetSet.

97



98 Figure 1: Locations of craters analyzed in this study (green circles). Background: Mars Orbiter Laser altimeter gridded data, where  
 99 white is high elevation and black is low elevation, credit MOLA Science Team/NASA/JPL.

100

### 101 3 Approach

#### 102 3.1 Identification of substrate

103 The substrate into which the gullies have incised is identified based on the following criteria:

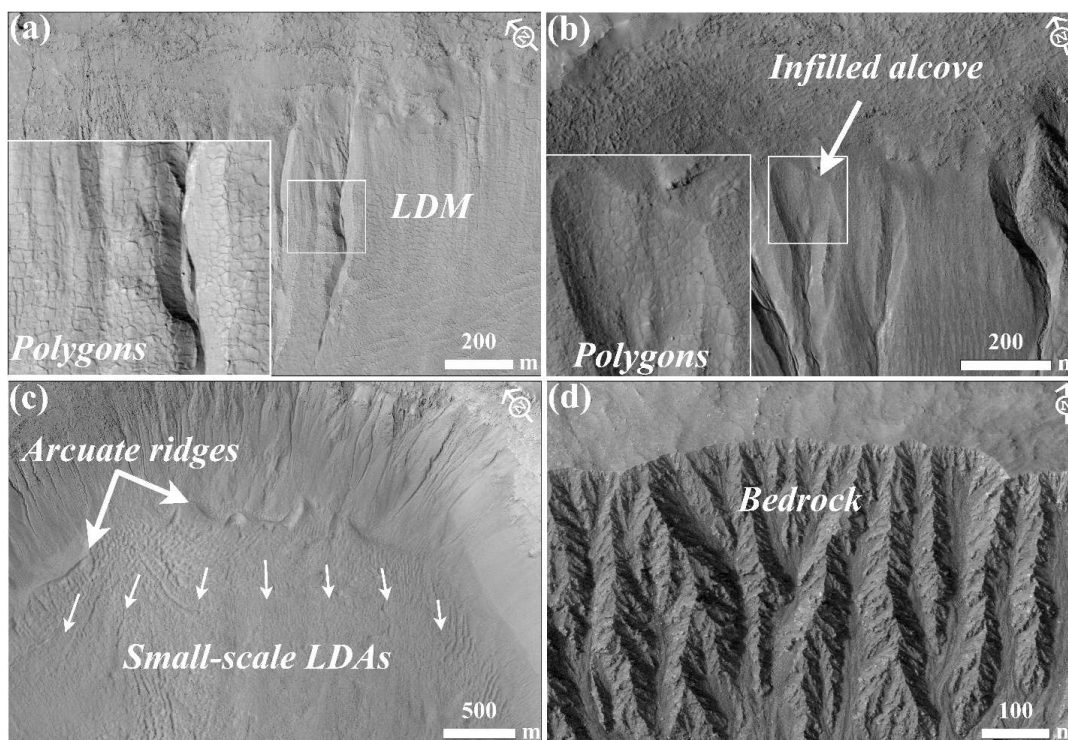
- 104 1. LDM/glacial deposits: Any crater whose gullies incise walls that appear to be softened by the drape of smooth mantling  
 105 material with polygonal cracks is inferred to have LDM as the substrate within which gullies have incised (e.g. Mustard et al.,  
 106 2001; Kreslavsky and Head, 2002; Levy et al., 2009a; Conway et al., 2018; de Haas et al., 2019a) (Fig. 2a). The alcoves on  
 107 the walls of these craters may be partially to completely filled by LDM, and in some cases, polygonized LDM materials may  
 108 be seen covering the alcove walls (e.g. Christensen, 2003; Conway et al., 2018; de Haas et al., 2019a). These infilled alcoves



109 on the crater walls are not the alcoves of gullies formed within the LDM substrate; instead, they represent the alcoves that were  
110 formed prior to the LDM emplacement epoch. Additionally, gullied craters that show evidence in the form of arcuate ridges at  
111 the foot of the walls and VFFs that cover part or the entire crater floor are inferred to have been modified by one or multiple  
112 episodes of glaciation (e.g. Arfstrom and Hartmann, 2005; Head et al., 2010; Milliken et al., 2003; Hubbard et al., 2011). These  
113 craters host gullies that are often partially or fully covered by LDM deposits.

114 2. Bedrock: Craters where the features listed in 1 are absent and where rocky material is visible extending downwards from  
115 the crater rim. This rocky material usually outcrops as spurs and can be layered or massive. The slopes can be smooth or  
116 covered with boulders, with concentrations of boulders at the slope toe.

117



118 **Figure 2:** Examples of morphological evidence used to identify LDM, glacial deposits, and bedrock. (a) Smooth mantling material  
119 inferred as LDM draped on the wall of Talu crater on the basis of polygonal cracks formed in the material. The bigger box is an  
120 expanded view of the polygons seen over the region outlined by the smaller box. (HiRISE image ESP\_011817\_1395). (b) An infilled  
121 alcove on the wall of an unnamed crater-2 in the Terra Sirenum. Evidence of polygons in the infilled material suggests presence of  
122 LDM deposits draped on the wall. The region shown in smaller box is expanded in the bigger box to show evidence of the polygons.  
123 (HiRISE image ESP\_020407\_1410). (c) Glaciation inferred in the Corozal crater on the basis of arcuate ridges formed at the foot of  
124 the crater wall and small-scale LDAs on the crater floor. Arrows indicate the downslope flow of LDAs on the floor. (HiRISE image





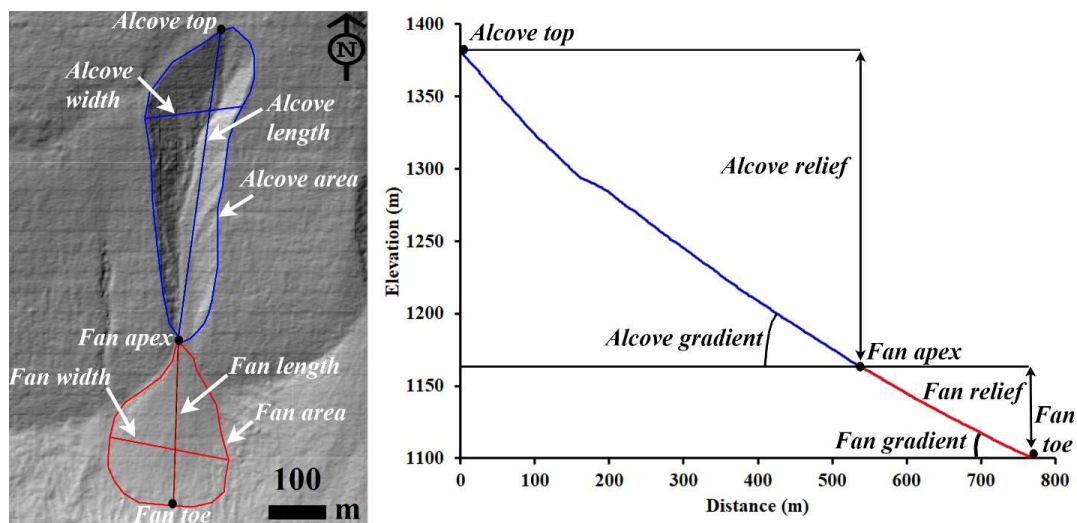
125 PSP\_006261\_1410). (d) Exposed fractured bedrock identified on the walls of Istok crater within which alcoves have incised. (HiRISE  
126 image ESP\_056668\_1345). HiRISE image credit: NASA/JPL /University of Arizona.

127

### 128 3.2 Morphometric variables

129 The measurements we made of each gully system include alcove area, alcove perimeter, alcove length, alcove width, alcove  
130 gradient, fan area, fan length, fan width, and fan gradient (Fig. 3). In total, we derived 18 morphometric variables to  
131 characterize each gully fan and its alcove. The morphometric variables are classified into geometry, relief, gradient, and  
132 dimensionless variables and they are calculated with established mathematical equations shown in Table 2. For the gradient  
133 measurement using the DTM, the topographic profile from (1) crest of the alcove to the apex of the fan was extracted for the  
134 alcove, and (2) apex to foot of the fan was extracted for the fan.

135



136 Figure 3: Examples of morphometric variables estimated in this work. Left panel: HiRISE DTM (Id:  
137 DTEEC\_002659\_1420\_002514\_1420) based hillshade. HiRISE DTM credit: NASA/JPL /University of Arizona. Right panel:  
138 Topographic profile: blue profile represents the topography of gully alcove from alcove top to fan apex and red profile represents  
139 the profile of gully fan from fan apex to fan toe.

140

141

142



143 **Table 2.** Set of morphometric variables extracted from the studied gully systems and their formulas and/or description of  
 144 method.

Morphometric variable	Formula and/or description of method	References
Alcove length and width	Measured in km	<b>Tomczyk, 2021</b>
Alcove area	Measured in km <sup>2</sup>	<b>Tomczyk, 2021</b>
Fan length and width	Measured in km	<b>Tomczyk, 2021</b>
Fan area	Measured in km <sup>2</sup>	<b>Tomczyk, 2021</b>
Melton ratio	(Alcove relief)/(Alcove area <sup>-0.5</sup> )	<b>Melton, 1957</b>
Relative concavity index	Concavity Index/(maximum relief between the uppermost and lowermost points along the gully fan profile/2). Concavity Index is estimated as $\sum (H_i^* - H_i) / N$ , where $H_i^*$ is the elevation along the straight line, $H_i$ is the elevation along the gully fan profile, $N$ is the total number of measurement points.	<b>Langbein, 1964; Phillips and Lutz, 2008</b>
Alcove gradient	Measured in (°)	<b>Tomczyk, 2021</b>
Fan gradient	Measured in (°)	<b>Tomczyk, 2021</b>
Alcove relief	Measured in km	<b>Tomczyk, 2021</b>
Fan relief	Measured in km	<b>Tomczyk, 2021</b>
Relief ratio (alcove and fan)	Alcove/fan relief divided by the length of the alcove/fan	<b>Schumm, 1956a, b</b>
Perimeter	Measured in km	<b>Schumm, 1956a, b</b>
Form factor	Alcove area divided by the square of the length of the alcove	<b>Horton, 1932</b>
Elongation ratio	Diameter of a circle of the same area as the alcove divided by the maximum alcove length	<b>Schumm, 1956a, b</b>
Circularity ratio	Alcove area divided by the area of the circle having the same perimeter as the alcove perimeter	<b>Miller, 1953</b>

145

### 146 3.3 Gully system selection for morphometric measurements

147 We have selected only those gully systems for morphometric measurements in which: (i) the depositional fan from an alcove-  
 148 channel system is not superimposed by or interfingering with the fans from the neighboring channels, (ii) there is clear  
 149 association between the primary channel emanating from the alcove that extends downslope and then deposit its respective  
 150 fan, (iii) no evidence of extensive cross-cutting is seen with the neighboring channels on the walls, (iv) no evidence of extensive  
 151 mantling by dust/aeolian deposits is apparent, and (v) no evidence of channel/fan superposition on any topographic obstacle  
 152 on the walls or the floor of the crater is apparent, which may eventually influence the morphometric measurements. Note that  
 153 the selection of the gully fans was also constrained by the coverage of HiRISE DTM that was used for morphometric analysis.



### 154 3.4 Statistical analysis of morphometric variables

155 We have two groups of gullies in our study: (1) gullies whose source area is incised into LDM/glacial deposits and (2) gullies  
156 whose source area is incised into the bedrock. At first, for both the groups we have calculated descriptive statistics for each of  
157 the morphometric variables shown in Table 2. The significance of the difference between the values of each of the  
158 morphometric variables calculated for each group was tested using a Student's t-test. To apply t-tests, we have transformed  
159 the morphometric variables to remove skewness by taking their natural logarithm. Correlation analysis has been used to  
160 investigate the correlation between the selected morphometric attributes of alcoves and fans. We infer strong positive  
161 correlations between variables if the correlation coefficient value is more than 0.7 and strong negative correlations if the value  
162 is less than -0.7. Very strong positive correlation between variables is inferred if the correlation coefficient is  $\geq 0.9$ . Further,  
163 we used canonical discriminant analysis (CDA) to determine morphometric variables that provide the most discrimination  
164 between the groups of gullies. In CDA, functions are generated according to the number of groups, until a number equal to n-  
165 1 functions is reached (n is the number of groups) (Conway et al., 2015). For the two groups of gullies in our study, there is  
166 going to be a function for which there is a standardised canonical discriminant function coefficient associated with the  
167 morphometric variable. The higher the magnitude of this coefficient for a particular morphometric variable, the higher the role  
168 of that variable in separating the groups of gullies. Standardisation was done by dividing each value for a given variable by  
169 the maximum value.

## 170 4 Results

### 171 4.1 Morphology of gully systems

172 Out of the 29 gullied craters analysed in this work, we have found that there are 24 craters influenced by LDM and VFFs. The  
173 remaining 5 craters have gullies incised into the exposed underlying bedrock on the wall of the crater. Below we describe the  
174 substrates identified in the studied craters and then compare the morphology of the gullies formed into those substrates.

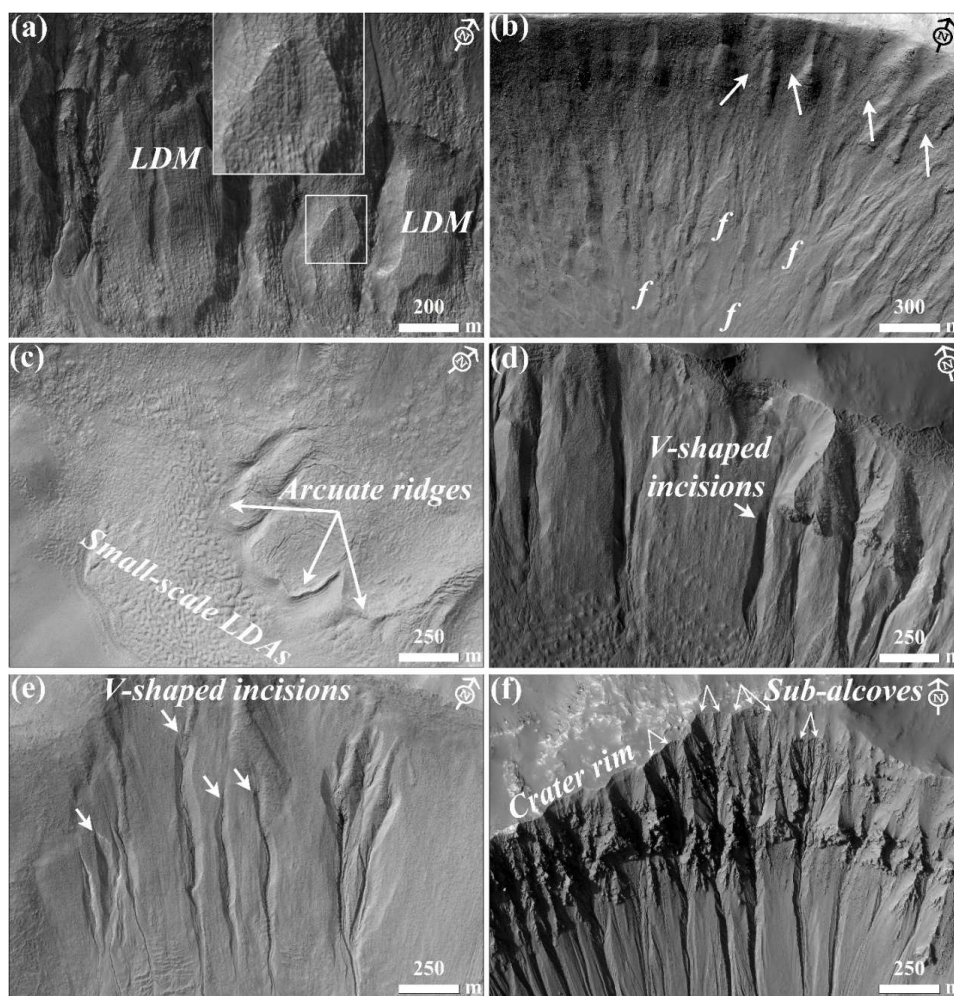
175 We found morphological evidence of LDM in the form of polygonized, smooth textured material on the pole-facing walls of  
176 4 craters namely Raga, Roseau, unnamed crater in Newton basin and unnamed crater-1 in Terra Sirenum. Morphological  
177 evidence of VFF is not evident in these craters. In these craters, the gully-alcoves and the gully-fan deposits both are covered  
178 by a smooth drape of polygonized LDM material. A typical example of this can be found in the unnamed crater formed inside  
179 the Newton basin (Fig. 4a). Roseau crater, in particular, contains a large number of pre-existing gully systems whose alcoves  
180 and fans are extensively mantled (Fig. 4b). Additionally, younger generation of gullies are visible that have incised within the  
181 LDM. The remaining 20 out of 24 craters contain evidence for gullies that specifically incised LDM as opposed to LDM that  
182 infills pre-existing alcoves and gullies, and influenced by VFFs (Table 1). The base of the pole-facing walls and the floor of  
183 the craters within which the gully systems have formed host linear-to-sinuuous arcuate ridges and VFFs, respectively. Typical  
184 examples of VFFs can be found in Corozal, Talu, unnamed craters in Terra Sirenum and Argyre basin, Langtang, Dechu and



185 Dunkassa craters (Fig. 4c). Gullies incised into LDM/VFFs are found to have a distinctive V-shaped cross section in their mid-  
186 section, they do not extend up to the crater rim, and often show multiple episodes of activity, inferred by the presence of fresh  
187 channel incision on the gully-fan surfaces (Fig. 4d-e).

188 Istok, Galap, Gasa, Los, and an unnamed crater in the Terra Sirenum contain gully systems on the pole-facing walls that are  
189 not associated with LDM and VFFs (Table 1). The alcoves inside these craters have a crenulated shape and appear to have  
190 formed by headward erosion into the bedrock of the crater rim (Fig. 4f). These craters have formed large gully systems on  
191 their pole-facing walls, with brecciated alcoves, comprising of multiple sub-alcoves and hosting many clasts/boulders (Fig.  
192 4f).

193  
194  
195  
196  
197  
198  
199  
200  
201  
202  
203  
204  
205  
206  
207  
208





209 **Figure 4: (a) LDM draped on the wall of an unnamed crater in the Newton basin. The inset shows details of the polygonal texture of**  
210 **the LDM. (HiRISE image PSP\_002686\_1410). (b) Infilled alcoves (arrows) and mantled fan surfaces (marked by letter ‘f’) on the**  
211 **wall of Roseau crater. (HiRISE image ESP\_024115\_1380). (c) Arcuate ridges at the foot of the crater wall and small-scale LDAs on**  
212 **the floor in Langtang crater. (HiRISE image ESP\_030099\_1415). (d) V-shaped incisions on the LDM draped walls of Taltal (HiRISE**  
213 **image ESP\_037074\_1400) and (e) Langtang crater (HiRISE image ESP\_030099\_1415). (f) Alcoves formed in Los crater by headward**  
214 **erosion into the crater rim. Individual alcoves formed in bedrock have multiple sub-alcoves. (HiRISE image ESP\_020774\_1445).**

215

#### 216 **4.2 Morphometry of gully systems**

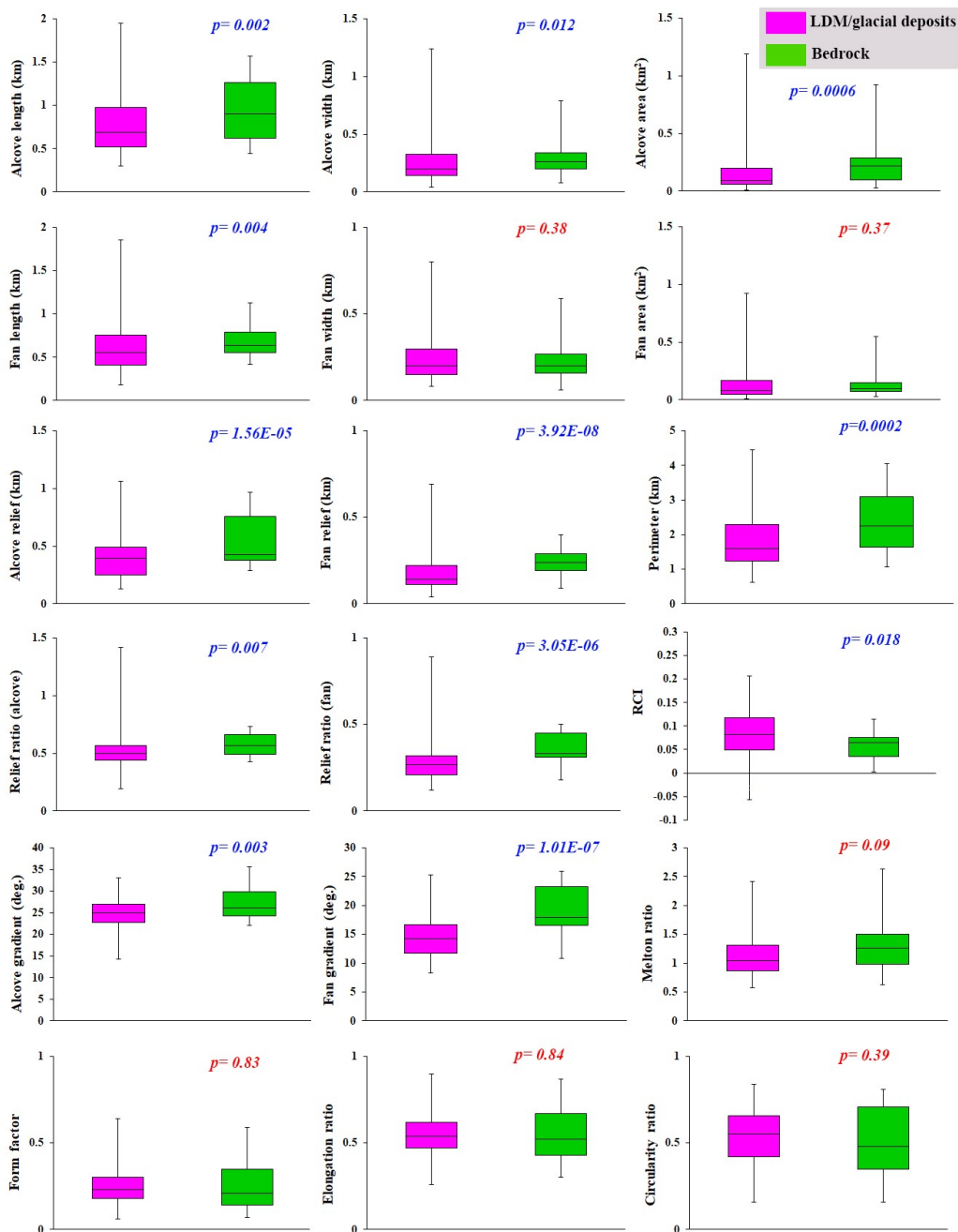
217 Based on the criteria summarized in section 3.3, we have studied 167 gullies across 29 craters for calculation of morphometric  
218 variables. 130 gullies are formed within LDM/glacial deposits, and 37 gullies are formed within the bedrock. The results of  
219 morphometric calculations are summarized for visual comparison as a boxplot (Fig. 5).

220 The results of the Student’s t-test indicates that all of the morphometric variables in Table 2, except fan width, fan area, melton  
221 ratio, form factor, elongation ratio, and circularity ratio, differ significantly between LDM/glacial deposits and bedrock (Fig.  
222 5). Compared to the mean gradient of gully-fans formed in LDM/glacial deposits, bedrock gully-fans are steeper and possess  
223 a higher relief ratio. The interquartile range of length, relief, and perimeter of alcoves formed in bedrock are also higher than  
224 the interquartile range of similar variables in LDM/glacial deposits, but the alcoves in LDM/glacial deposits possess much  
225 higher values of length, relief, and perimeter (Fig. 5).

226



227





228

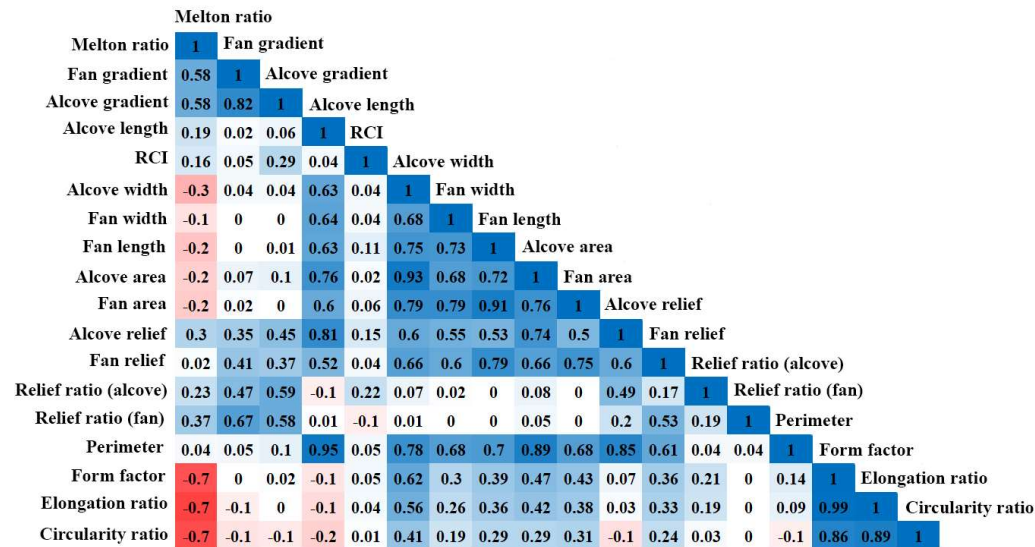
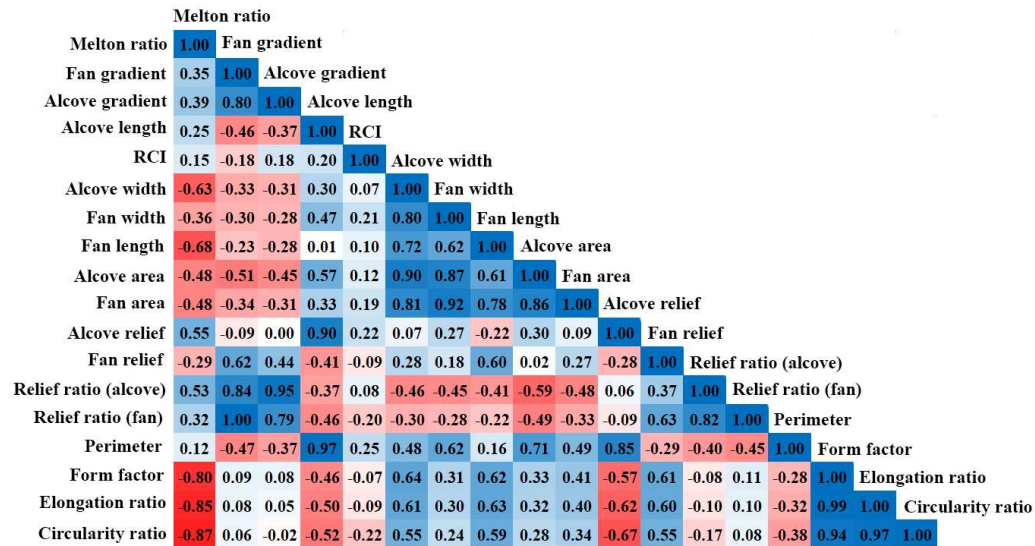
229 **Figure 5: Boxplots showing the range of values of alcove/fan geometry, relief, gradient, and dimensionless variables of gullies incised**  
230 **into LDM/glacial deposits (pink) and bedrock (green). P-values on the plots represent the results of the student's t-tests for testing**  
231 **the significance of difference in means of the morphometric variables between gully systems formed on LDM/Glacial deposits and**  
232 **bedrock. P-values in blue correspond to significant difference (with respect to a p-value of 0.05) and those in red are non-significant.**

233

234 Correlations between morphometric attributes of alcoves and fans formed in bedrock and LDM/glacial deposits are  
235 summarized in Fig. 6. For bedrock, there are strong positive correlations between 12 pairs of morphometric variables and  
236 strong negative correlations between 3 pairs of morphometric variables. For LDM/glacial deposits, there are strong positive  
237 correlations between 18 pairs of morphometric variables and strong negative correlations between 3 pairs of morphometric  
238 variables. Very strong positive correlations are found between 9 pairs of morphometric variables for bedrock and between 4  
239 pairs of morphometric variables for LDM/glacial deposits.



240







241 **Figure 6: Correlations between morphometric attributes of alcoves and fans formed in (a) bedrock and (b) LDM/glacial deposits.**  
242 **Higher the value of the correlation coefficient, higher is the strength of the correlation.**

243

244 The canonical discriminant analysis reveals that the following morphometric variables best distinguish between the gully  
245 systems formed in LDM/glacial deposits and bedrock, in descending order of importance: alcove perimeter, alcove relief, fan  
246 gradient, fan relief, fan length, relief ratio (alcove), alcove width, relief ratio (fan), alcove gradient, alcove area, alcove length,  
247 and relative concavity index (Table 3). The alcove perimeter is most important in discriminating among the gully systems  
248 formed within LDM/glacial deposits and bedrock, and the next two most important variables are alcove relief and fan gradient.  
249 Alcove relief and fan gradient have 4/5 and 1/3 the weight of alcove perimeter, respectively. The remaining variables such as  
250 fan relief, fan length, relief ratio (alcove), alcove width, and relief ratio (fan) have nearly 1/5 the weight of alcove perimeter  
251 or greater (but less than 1/3) discriminatory power in separating between the gullies formed in LDM/glacial deposits and  
252 bedrock. The variables with the smallest magnitude, alcove gradient, alcove area, alcove length and relative concavity index,  
253 have less than 1/10 the weight of the most important variable in separating the gully systems.

254 **Table 3.** Standardised canonical discriminant function coefficients (F1) that best separate gully systems formed on  
255 LDM/Glacial deposits and bedrock.

Variable	F1
Perimeter	3.552
Alcove relief	-2.828
Fan gradient	1.278
Fan length	-1.06
Fan relief	1.06
Relief ratio (alcove)	0.971
Alcove width	-0.692
Relief ratio (fan)	-0.665
Alcove gradient	-0.331
Alcove area	-0.319
Alcove length	0.23
Relative concavity index	-0.182

256



## 257 5 Discussions

### 258 5.1 Unique morphology and morphometry of gully systems in different substrates

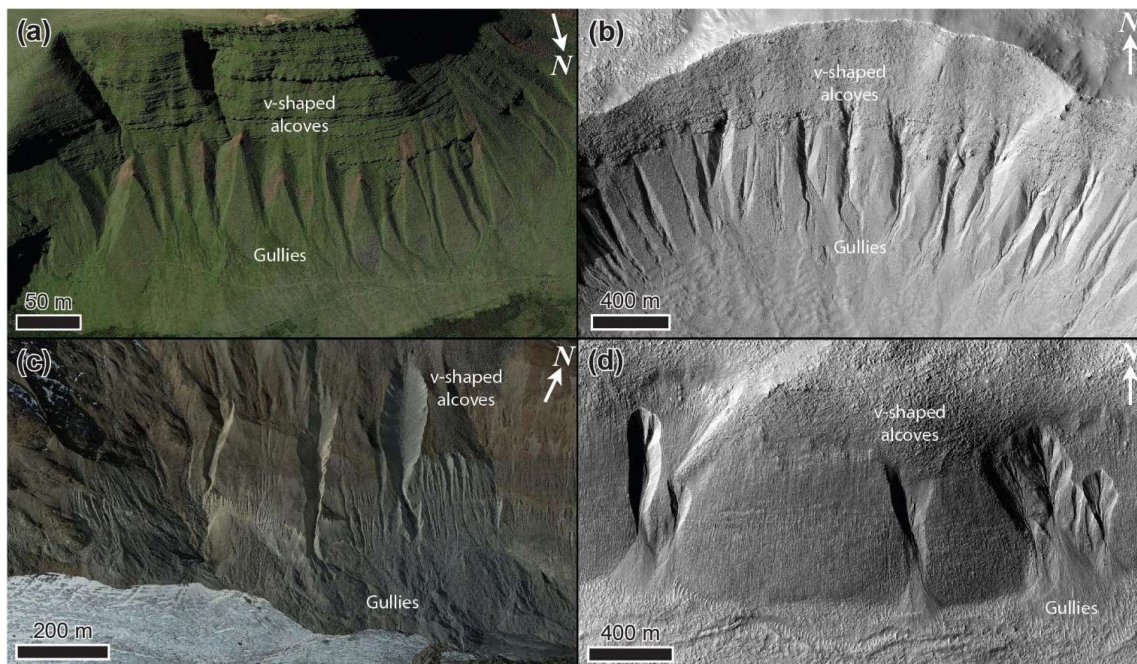
259 We have found that the gully systems formed in LDM/glacial deposits and bedrock can, using discriminatory analysis, be  
260 distinguished from one another in terms of perimeter and relief of alcoves (Table 3). Additionally, we have found statistically  
261 significant difference between the perimeter and relief of alcoves formed in LDM/glacial deposits and bedrock (Fig. 5). It is  
262 likely that these differences in the perimeter and relief of alcoves formed within morphologically distinct substrates could be  
263 due to the integral nature of the surface material within which the alcoves have formed. In other words, it is possible that the  
264 differences in the physical properties of the sediments (viz. grain size, compactness etc.) within which alcoves have formed  
265 played a key role in erosion of the substrate leading to differences in their morphometric variables. Below we elaborate on the  
266 uniqueness of the substrates within which alcoves have formed, and discuss further the relationships between the morphometric  
267 variables of the morphologically distinct gully systems.

268 On Mars, VFFs contain high purity glacial ice with a debris cover (Sharp, 1973; Squyres, 1978, 1979; Squyres and Carr, 1986;  
269 Holt et al 2008, Plaut et al 2009, Petersen et al. 2018). Their surfaces have been interpreted to be comprised of finer, reworked  
270 debris derived from sublimation of the underlying ice (Mangold, 2003; Levy et al., 2009a; Morgan et al., 2009). The smooth,  
271 meters thick draping unit on the walls of formerly glaciated craters has been suggested to be derived from the atmosphere as a  
272 layer of dust-rich ice primarily constituting of fine-grained materials (Kreslavsky and Head, 2000; Mustard et al., 2001). The  
273 fine-grained materials are loosely-packed, unconsolidated materials exhibiting low thermal inertia values (Mellon et al., 2000;  
274 Putzig et al., 2005). Typically, gullies formed within this substrate display a smooth surface texture, wherein, evidence of  
275 individual clasts or meter-scale boulders is not resolvable in HiRISE images, substantiating the dominant component of fine-  
276 grained materials within the LDM (e.g., Levy et al., 2010; de Haas et al., 2015a). Additionally, it has been found that alcoves  
277 incised into the LDM always have a distinctive V-shaped cross section in their mid-section, which when compared with  
278 similar-scaled systems on Earth also corresponds to the presence of loose sediments constituting the LDM (Conway et al.,  
279 2018). The alcoves with V-shaped cross sections are found to be elongated, likely indicating incision within ice-rich unlithified  
280 sediments (Aston et al., 2011). In the studied craters, we have found that gullies incised into LDM/glacial deposits are having  
281 an elongated, V-shaped cross section in their mid-section (Fig. 4). We propose that the presence of fine-grained, loosely  
282 packed, unconsolidated materials within LDM/glacial deposits has facilitated formation of elongated alcoves with perimeter  
283 and relief relatively higher than that of alcoves formed in coarse-grained bedrock substrate. This is consistent with the previous  
284 studies suggesting that gullies eroding into LDM/glacial deposits have elongated catchments, whereas gullies eroding into the  
285 bedrock have more amphitheater-shaped catchments (Levy et al., 2009b). For this reason, the estimated length of alcoves  
286 formed in LDM/glacial deposits is found to be relative higher than that of alcoves formed in bedrock (Fig. 5). Furthermore,  
287 statistical analysis has revealed a significant difference between the length of alcoves formed in LDM/glacial deposits and  
288 bedrock (Fig. 5). Additionally, the presence of finer-grained sediments in LDM/glacial deposits is the likely cause of the V-



289 shape of the incision of alcoves investigated in this study (Aston et al., 2011). On Earth, V-shaped incisions through glacial  
290 ice-rich moraines have been observed to have occurred during the paraglacial phase of glacial retreat (Bennett et al., 2000;  
291 Ewertowski and Tomczyk, 2015) (Fig. 7). The paraglacial phase refers to a terrestrial post-glacial period that represents the  
292 response of changing environment to deglaciation (Bennett et al., 2000; Ewertowski and Tomczyk, 2015).

293



294

295 **Figure 7: Gullies forming in glacial sediments in deglaciated terrain in the (a) Brecon Beacons, Wales, UK on Earth (Google Earth**  
296 **coordinates: 51°52'59.11"N, 3°43'33.26"W), (b) Talu crater ([https://www.uahirise.org/ESP\\_011817\\_1395](https://www.uahirise.org/ESP_011817_1395)) on Mars, (c)**  
297 **Hintereisferner, Austria (Google Earth coordinates: 46°48'54.25"N, 10°47'8.18"E), on Earth, and (d) Bunnik crater**  
298 **([https://www.uahirise.org/ESP\\_047044\\_1420](https://www.uahirise.org/ESP_047044_1420)) on Mars. HiRISE image credit: NASA/JPL-Caltech/University of Arizona.**

299

300 The next most important difference between these two types of gullies is the mean gradient of gully fans. At the foot of the  
301 fans, mean gradient of the fans influenced by LDM/glacial deposits is  $<15^\circ$  for 61% of the studied fans. For bedrock, 84% of  
302 the studied fans have a mean gradient  $>15^\circ$  at the foot of the fans. Hence, gully-fans formed in bedrock are emplaced at a



303 relatively steeper gradient than the fans formed from gullies in LDM/glacial deposits. We propose that the nature of the material  
304 mobilized can explain this difference, with the finer-grained sediments characteristic of the LDM/glacial type gullies being  
305 easier to mobilise and being entrained to lower slope angles, than the coarser sediments found within the bedrock type gullies.

## 306 **5.2 Evaluation of the gully formation process**

307 On Earth, alcove-fan systems can roughly be subdivided in flood-dominated, debris-flow dominated, and colluvial systems.  
308 Following the terminology of De Haas et al., (2015b) and Tomczyk (2021), we define these systems as follows:

309 1) Flood-dominated systems: These are systems dominated by fluid-gravity flows, i.e., water floods, hyperconcentrated floods,  
310 and debris floods. The fans of such systems are commonly referred to as fluvial or alluvial fans (e.g., Ryder, 1971; Blair and  
311 McPherson, 1994; Hartley et al., 2005).

312 2) Debris-flow dominated systems: These are systems dominated by sediment-gravity flows, i.e., debris flows, mud flows.  
313 Irrespective of their radial extent and depositional gradients, the fans aggraded by these systems can be commonly called  
314 debris-flow fans or debris fans (Blikra and Nemeč, 1998; de Scally et al., 2010).

315 3) Colluvial systems: These are systems dominated by rock-gravity and sediment-gravity flows, with their dominant activity  
316 relating to rockfalls, grain flows, and snow avalanches (in periglacial and alpine settings). Debris flows typically constitute  
317 only a relatively minor component of geomorphic processes in such systems. The fans of these systems are also commonly  
318 known as colluvial cones or talus cones (Siewert et al., 2012; De Haas et al., 2015b).

319 Although these systems may be dominated by one type of geomorphic process, it is important to stress that other processes  
320 may also occur. For example, on Earth water floods are not uncommon on many debris-flow dominated systems, while debris-  
321 flow deposits are commonly recognized on colluvial cones.

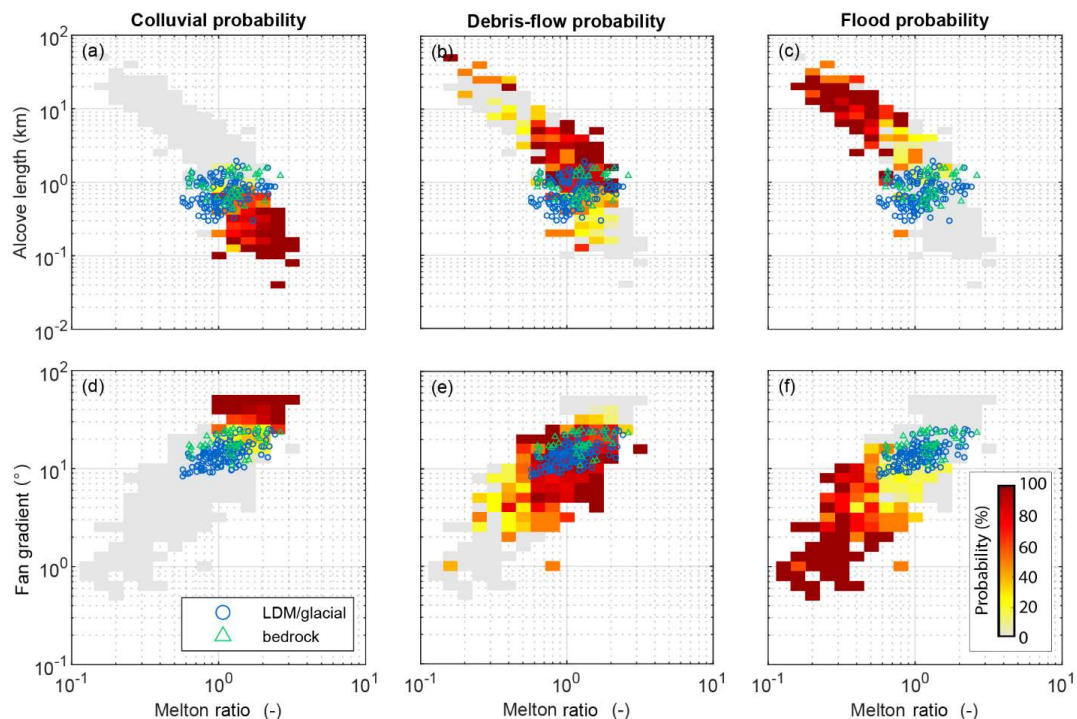
322

323

324



325



326

327 **Figure 8: Comparison of combinations of Melton ratio with Alcove length and Fan gradient. The probability heat maps**  
328 **are based on previously published data – see text for references. The Martian gully systems formed in LDM/glacial**  
329 **deposits and bedrock are found to be in the debris-flow regime on Earth.**

330

331 To compare the morphometric characteristics of the Martian gully systems to terrestrial systems, we have compiled  
332 morphometric data of alcoves and fans across several continents, mountain ranges, climate zones, and process types on Earth.  
333 This dataset includes published data from the Himalayas, Ladakh, India (Stolle et al., 2013), the tropical Andes, Columbia  
334 (Arango et al., 2021), Spitsbergen, Svalbard (Tomczyk, 2021), British Columbia, Canada (Kostaschuk, 1986; Jackson et al.,  
335 1987; and newly presented data), the southern Carpathians, Romania (Ilinca et al., 2021), the Southern Alps, New Zealand (De  
336 Scally and Owens, 2004; De Scally et al., 2010), the North Cascade Foothills, USA, the European Alps (including Switzerland,  
337 Italy, France, and Austria), and the Pyrenees (from multiple authors compiled by Bertrand et al., 2013). The dataset comprises  
338 information from colluvial, debris-flow, and flood (also including debris flood) dominated systems. In total, it contains 231



339 colluvial systems, 749 debris-flow dominated systems, and 369 flood-dominated systems. In total, data were compiled for  
340 1349 systems, although not all information was available for all systems, with data availability ranging from 729 sites for  
341 alcove length to all 1349 systems for Melton index and process type. Based on this data we have made a heatmap of the  
342 probability of flood, debris-flow, or colluvially-dominated conditions for combinations of Melton ratio with alcove length and  
343 fan gradient, to which we compare the Martian gullies (Fig. 8). We have found that the Martian gullies are indeed in the debris-  
344 flow regime on Earth. Moreover, they are closer to the transition to the smaller and steeper colluvial cones than to transition  
345 to flood-dominated fans. As expected, bedrock systems in Fig. 8d-e are closer to the colluvial systems than the LDM systems.

346

347 According to the previous reports of debris-flow like deposits found in Martian gullies (e.g. Johnsson et al., 2014; Sinha et al.,  
348 2019, 2020), the morphological attributes of debris-flow like deposits typically include overlapping tongue-shaped lobes with  
349 embedded clasts, channels with medial deposits, and channels with clearly defined lateral levees. Although it is still not clear  
350 whether the formation of these deposits in gullies are from sublimation of CO<sub>2</sub> ice or due to meltwater generation. De Haas et  
351 al., (2019b) showed that CO<sub>2</sub> sublimation may lead to flow fluidization on Mars in a manner similar to fluidization by water  
352 in terrestrial debris flows; a concept supported by the recent finding of lobate deposits and boulder-rich levee formation during  
353 the present-day in Istok crater (Table 1) (Dundas et al., 2019). The formation of these morphologically similar deposits during  
354 the present-day is attributed to sublimating CO<sub>2</sub> frost, which likely produces the necessary fluidization likely by gas generated  
355 from entrained CO<sub>2</sub> frost (Dundas et al., 2019). On the basis of these recent reports (De Haas et al., 2019b; Dundas et al., 2019)  
356 and based on our own findings in this study, we argue that a debris-flow like process similar to those operated in the terrestrial  
357 gully systems has likely dominated the flow types that lead to gully formation on Mars.

## 358 **6 Conclusions**

359 This paper compares morphological and morphometric characteristics of gully alcoves and associated fans formed in  
360 LDM/glacial deposits and bedrock over walls of 29 craters between 30° S and 75° S latitudes. 5 craters out of 29 have alcoves-  
361 fans formed within the bedrock and remaining 24 craters have alcoves-fans formed within LDM/glacial deposits. From our  
362 analysis of 167 gullies, we posit that gully systems formed in LDM/glacial deposits and bedrock differ from one another using  
363 the following lines of evidence:

- 364 • Alcoves formed in LDM/glacial deposits are more elongated than the alcoves formed in bedrock, and possess a distinctive  
365 V-shaped cross section.
- 366 • The mean gradient of gully-fans formed in bedrock is steeper than the mean gradient of fans formed from gullies in  
367 LDM/glacial deposits.



368 Based on the combinations of Melton ratio with alcove length and fan gradient, we suggest that the gully systems studied in  
369 this work were likely dominated by terrestrial debris-flow like processes during their formation. This is consistent with the  
370 findings reported in previous studies that showed evidence of formation of deposits morphologically similar to terrestrial  
371 debris-flow like deposits, both in the past and during the present-day (e.g., Johnsson et al., 2014; Dundas et al., 2019). The  
372 present-day sublimation of CO<sub>2</sub> ice on Mars is envisaged to provide the necessary flow fluidization for the emplacement of  
373 deposits similar to debris-flow like deposits on Earth (De Haas et al., 2019b).

#### 374 **7 Author contribution**

375 RKS, TDH and SJC conceptualized this work. The methodology was developed by RKS, TDH and SJC. Data curation and  
376 formal analyses were performed by RKS. TDH and AN also contributed in collection of datasets used in this work. RKS, DR,  
377 TDH and SJC contributed to the interpretation of the data and results. RKS wrote the original draft of this paper, which was  
378 reviewed and edited by all authors.

#### 379 **8 Conflict of interest**

380 SJC is a Guest Editor of this special issue (Planetary landscapes, landforms, and their analogues) of ESurfD and on the editorial  
381 board for ESurf. The peer-review process was guided by an independent editor, and the authors have also no other competing  
382 interests to declare.

#### 383 **9 Acknowledgements**

384 We would like to thank the HiRISE team for their work to produce the images and digital elevation models used in this study,  
385 it would have been impossible without them. RKS and DR acknowledge the financial support by the Indian Space Research  
386 Organisation, Department of Space, Government of India. SJC and AN are grateful for the financial support from Région Pays  
387 de la Loire, project étoiles montantes METAFLOWS (convention N° 2019-14294) and also the financial support of CNES in  
388 support of their HiRISE work. TdH was supported by the Netherlands Organisation for Scientific Research (NWO) (grant  
389 016.Veni.192.001). We acknowledge the efforts of team MUTED to develop an online tool (<http://muted.wwu.de/>) for quick  
390 identification of the spatial and multi-temporal coverage of planetary image data from Mars. All the planetary datasets used in  
391 this work are available for free download at the PDS Geosciences Node Mars Orbital Data Explorer (ODE)  
392 (<https://ode.rsl.wustl.edu/mars/>) and <https://www.uahirise.org/>. The newly-generated DTMs can be downloaded from  
393 [https://figshare.com/articles/dataset/Self\\_generated\\_DEMs/21717164](https://figshare.com/articles/dataset/Self_generated_DEMs/21717164). The measurement datasets can be downloaded from  
394 [https://figshare.com/articles/dataset/Measurement\\_data\\_of\\_gully\\_systems\\_in\\_the\\_southern\\_mid\\_latitudes\\_of\\_Mars/](https://figshare.com/articles/dataset/Measurement_data_of_gully_systems_in_the_southern_mid_latitudes_of_Mars/21717182)  
395 **21717182**. This work is a part of the PhD work of Rishitosh K. Sinha. Director PRL, Head of Planetary Science Division,



396 PRL, Head of Planetary Remote Sensing Section, PRL, and Director IIT Gandhinagar are gratefully acknowledged for constant  
397 encouragement during the work.

## 398 References

- 399 Arango, M. I., Aristizábal, E., & Gómez, F.: Morphometrical analysis of torrential flows-prone catchments in tropical and  
400 mountainous terrain of the Colombian Andes by machine learning techniques, *Natural Hazards*, 105(1), 983–1012, doi:  
401 <https://doi.org/10.1007/s11069-020-04346-5>, 2021.
- 402 Arfstrom, J. & Hartmann, W.K.: Martian flow features, moraine-like ridges, and gullies: terrestrial analogs and  
403 interrelationships, *Icarus*, 174, 321–335, doi: <https://doi.org/10.1016/j.icarus.2004.05.026>, 2005.
- 404 Aston, A., Conway, S. & Balme, M.: Identifying Martian Gully Evolution. In: Balme, M.R., Bargery, A.S., Gallagher, C.J. &  
405 Gupta, S. (eds) *Martian Geomorphology*, Geological Society, London, Special Publications, 356, 151–169, doi:  
406 <https://doi.org/10.1144/SP356.9>, 2011.
- 407 Balme, M., Mangold, N. Et Al.: Orientation and distribution of recent gullies in the southern hemisphere of Mars: observations  
408 from High Resolution Stereo Camera/Mars Express (HRSC/MEX) and Mars Orbiter Camera/Mars Global Surveyor  
409 (MOC/MGS) data, *J. Geophys. Res.: Planets*, 111, E05001, doi: <https://doi.org/10.1029/2005JE002607>, 2006.
- 410 Bertrand, M., Liébault, F., & Piégay, H.: Debris-flow susceptibility of upland catchments, *Natural Hazards*, 67(2), 497–511,  
411 doi: <https://doi.org/10.1007/s11069-013-0575-4>, 2013.
- 412 Blair, T.C. & McPherson, J.G.: Processes and forms of alluvial fans. In: PARSONS, A. & ABRAHAMS, A. (eds)  
413 *Geomorphology of Desert Environments*, Springer, Dordrecht, The Netherlands, 413–467, doi: [https://doi.org/10.1007/978-1-](https://doi.org/10.1007/978-1-4020-5719-9_14)  
414 [4020-5719-9\\_14](https://doi.org/10.1007/978-1-4020-5719-9_14), 2009.
- 415 Blair, T.C.: Sedimentology of the debris-flow-dominated Warm Spring Canyon alluvial fan, Death Valley, California,  
416 *Sedimentology* 46 (5), 941–965, doi: <https://doi.org/10.1046/j.1365-3091.1999.00260.x>, 1999.
- 417 Blikra, L.H., Nemeč, W.: Postglacial colluvium in western Norway: depositional processes, facies and palaeoclimatic record.  
418 *Sedimentology* 45 (5), 909–960, doi: <https://doi.org/10.1046/j.1365-3091.1998.00200.x>, 1998.
- 419 Cedillo-Flores, Y., Treiman, A.H., Lasue, J. & Clifford, S.M.: CO<sub>2</sub> gas fluidization in the initiation and formation of Martian  
420 polar gullies, *Geophys. Res. Letters*, 38, L21202 doi: <https://doi.org/10.1029/2011GL049403>, 2011.
- 421 Christensen, P.R.: Formation of recent Martian gullies through melting of extensive water-rich snow deposits, *Nature*, 422,  
422 45–48, doi: <https://doi.org/10.1038/nature01436>, 2003.





- 423 Conway, S. J., Butcher, F. E., de Haas, T., Deijns, A. A., Grindrod, P. M., & Davis, J. M.: Glacial and gully erosion on Mars:  
424 A terrestrial perspective, *Geomorphology*, 318, 26-57, doi: <https://doi.org/10.1016/j.geomorph.2018.05.019>, 2018.
- 425 Conway, S.J. & Balme, M.R.: Decameter thick remnant glacial ice deposits on Mars, *Geophys. Res. Letters*, 41, 5402–5409,  
426 doi: <https://doi.org/10.1002/2014GL060314>, 2014.
- 427 Conway, S.J., Balme, M.R., Kreslavsky, M.A., Murray, J.B. & Towner, M.C.: The comparison of topographic long profiles  
428 of gullies on Earth to gullies on Mars: a signal of water on Mars. *Icarus*, 253, 189–204, doi:  
429 <https://doi.org/10.1016/j.icarus.2015.03.009>, 2015.
- 430 Conway, S.J., Balme, M.R., Murray, J.B., Towner, M.C., Okubo, C.H. & Grindrod, P.M.: The indication of Martian gully  
431 formation processes by slope–area analysis, In: Balme, M.R., Bargery, A.S., Gallagher, C.J. & Gupta, S. (eds) *Martian*  
432 *Geomorphology*, Geological Society, London, Special Publications, 356, 171–201, doi: <https://doi.org/10.1144/SP356.10>,  
433 2011.
- 434 Conway, S.J., Harrison, T.N., Soare, R.J., Britton, A.W. & Steele, L.J.: New slope-normalized global gully density and  
435 orientation maps for Mars, In: Conway, S.J., Carrivick, J.L., Carling, P.A., De Haas, T. & Harrison, T.N. (eds) *Martian Gullies*  
436 *and their Earth Analogues*, *Geol. Soc. Lond. Spec. Publ.* 467. First published online November 27, 2017, doi:  
437 <https://doi.org/10.1144/SP467.3>, 2017.
- 438 Costard, F., Forget, F., Mangold, N. & Peulvast, J.P.: Formation of recent Martian debris flows by melting of near-surface  
439 ground ice at high obliquity, *Science*, 295, 110–113, doi: [10.1126/science.1066](https://doi.org/10.1126/science.1066), 2002.
- 440 Crosta, G.B., Frattini, P.: Controls on modern alluvial fan processes in the central Alps, northern Italy, *Earth Surf. Proc. Land*.  
441 29 (3), 267–293, doi: <https://doi.org/10.1002/esp.1009>, 2004.
- 442 de Haas, T., Conway, S.J., Butcher, F.E.G., Levy, J.S., Grindrod, P.M., Balme, M.R., Goudge, T.A.: Time will tell: temporal  
443 evolution of Martian gullies and paleoclimatic implications, *Geol. Soc. Lond. Spec. Publ.* 467, doi:  
444 <https://doi.org/10.1144/SP467.1>, 2019a.
- 445 de Haas, T., McArdell, B. W., Conway, S. J., McElwaine, J. N., Kleinhans, M. G., Salese, F., & Grindrod, P. M.: Initiation  
446 and flow conditions of contemporary flows in Martian gullies, *J. Geophys. Res.: Planets*, 124(8), 2246-2271, doi:  
447 <https://doi.org/10.1029/2018JE005899>, 2019b.
- 448 de Haas, T., Hauber, E. & Kleinhans, M.G. 2013. Local late Amazonian boulder breakdown and denudation rate on Mars,  
449 *Geophys. Res. Letters*, 40, 3527–3531, doi: <https://doi.org/10.1002/grl.50726>, 2013.
- 450 de Haas, T., Ventra, D., Hauber, E., Conway, S.J. & Kleinhans, M.G.: Sedimentological analyses of Martian gullies: the  
451 subsurface as the key to the surface, *Icarus*, 258, 92–108, doi: <https://doi.org/10.1016/j.icarus.2015.06.017>, 2015a.



- 452 de Haas, T., Kleinhans, M. G., Carbonneau, P. E., Rubensdotter, L., & Hauber, E.: Surface morphology of fans in the high-  
453 Arctic periglacial environment of Svalbard: Controls and processes, *Earth-Science Reviews*, 146, 163-182, doi:  
454 <https://doi.org/10.1016/j.earscirev.2015.04.004>, 2015b.
- 455 de Scally, F. A., & Owens, I. F.: Morphometric controls and geomorphic responses on fans in the Southern Alps, New Zealand,  
456 *Earth Surface Processes and Landforms: The Journal of the British Geomorphological Research Group*, 29(3), 311-322, doi:  
457 <https://doi.org/10.1002/esp.1022>, 2004.
- 458 De Scally, F.A., Owens, I.F., Louis, J.: Controls on fan depositional processes in the schist ranges of the Southern Alps, New  
459 Zealand, and implications for debris-flow hazard assessment, *Geomorphology* 122 (1–2), 99–116, doi:  
460 <https://doi.org/10.1016/j.geomorph.2010.06.002>, 2010.
- 461 Dickson, J.L. & Head, J.W.: The formation and evolution of youthful gullies on Mars: gullies as the latestage phase of Mars  
462 most recent ice age, *Icarus*, 204, 63–86, doi: <https://doi.org/10.1016/j.icarus.2009.06.018>, 2009.
- 463 Dickson, J.L. et al.: Recent climate cycles on Mars: Stratigraphic relationships between multiple generations of gullies and the  
464 latitude dependent mantle, *Icarus* 252, 83–94, doi: <http://dx.doi.org/10.1016/j.icarus.2014.12.035>, 2015.
- 465 Dickson, J.L., Head, J.W., Fassett, C.I.: Patterns of accumulation and flow of ice in the mid-latitudes of Mars during the  
466 Amazonian, *Icarus* 219, 723–732, doi: <http://dx.doi.org/10.1016/j.icarus.2012.03.010>, 2012.
- 467 Dickson, J.L., Head, J.W., Kreslavsky, M.: Martian gullies in the southern midlatitudes of Mars: Evidence for climate-  
468 controlled formation of young fluvial features based upon local and global topography, *Icarus* 188, 315–323, doi:  
469 <https://doi.org/10.1016/j.icarus.2006.11.020>, 2007.
- 470 Dundas, C. M., McEwen, A. S., Diniega, S., Hansen, C. J., Byrne, S., & McElwaine, J. N.: The formation of gullies on Mars  
471 today, *Geol. Soc. Lond. Spec. Publ.* 467, 67-94, doi: <https://doi.org/10.1144/SP46>, 2019.
- 472 Dundas, C.M., Diniega, S., Hansen, C.J., Byrne, S., McEwen, A.S.: Seasonal activity and morphological changes in martian  
473 gullies, *Icarus* 220:124–143, doi: <https://doi.org/10.1016/j.icarus.2012.04.005>, 2012.
- 474 Dundas, C.M., Diniega, S., McEwen, A.S.: Long-term monitoring of Martian gully formation and evolution with  
475 MRO/HiRISE, *Icarus* 251:244–263, doi: <https://doi.org/10.1016/j.icarus.2014.05.013>, 2015.
- 476 Harrison, T.N., Osinski, G.R., Tornabene, L.L., Jones, E.: Global documentation of gullies with the Mars reconnaissance  
477 orbiter context camera and implications for their formation, *Icarus* 252:236–254, doi:  
478 <https://doi.org/10.1016/j.icarus.2015.01.022>, 2015.



- 479 Hartley, A.J., Mather, A.E., Jolley, E., Turner, P.: Climatic controls on alluvial-fan activity, Coastal Cordillera, northern Chile.  
480 In: Harvey, A.M., Mather, A.E., Stokes, M. (Eds.), Alluvial Fans: Geomorphology, Sedimentology, Dynamics. Geol. Soc.  
481 Lond. Spec. Publ. 251, 95-115, doi: <https://doi.org/10.1144/GSL.SP.2005.251.01.>, 2005.
- 482 Head, J.W., Marchant, D.R., Dickson, J.L., Kress, A.M., Baker, D.M.: Northern midlatitude glaciation in the Late Amazonian  
483 period of Mars: criteria for the recognition of debris-covered glacier and valley glacier landsystem deposits, Earth Planet. Sci.  
484 Lett. 294:306–320, doi: <https://doi.org/10.1016/j.epsl.2009.06.041>, 2010.
- 485 HELDMANN, J.L. & MELLON, M.T.: Observations of Martian gullies and constraints on potential formation mechanisms,  
486 Icarus, 168, 285–304, doi: <https://doi.org/10.1016/j.icarus.2003.11.024>, 2004.
- 487 Heldmann, J.L. et al.: Formation of martian gullies by the action of liquid water flowing under current martian environmental  
488 conditions, J. Geophys. Res. Planets 110, doi: <http://dx.doi.org/10.1029/2004JE002261>, 2005.
- 489 Hobbs, S.W., Paull, D.J., Clark, J.D.A.: A comparison of semiarid and subhumid terrestrial gullies with gullies on Mars:  
490 Implications for martian gully erosion, Geomorphology 204, 344–365, doi: <http://dx.doi.org/10.1016/j.geomorph.2013.08.018>,  
491 2014.
- 492 Hobbs, S.W., Paull, D.J. and Clarke, J.D.A.: Analysis of regional gullies within Noachis Terra, Mars: A complex relationship  
493 between slope, surface material and aspect, Icarus, 250, 308-331, doi: <https://doi.org/10.1016/j.icarus.2014.12.011>, 2015.
- 494 Hubbard, B., Milliken, R.E., Kargel, J.S., Limaye, A. & Souness, C.: Geomorphological characterisation and interpretation of  
495 a mid-latitude glacier-like form: Hellas Planitia, Mars, Icarus, 211, 330–346, doi: <https://doi.org/10.1016/j.icarus.2010.10.021>,  
496 2011.
- 497 Ilinca, V.: Using morphometrics to distinguish between debris flow, debris flood and flood (Southern Carpathians, Romania),  
498 Catena, 197, 104982, doi: <https://doi.org/10.1016/j.catena.2020.104982>, 2021.
- 499 Jackson LE, Kostaschuk RA, MacDonald GM: Identification of debris flow hazard on alluvial fans in the Canadian Rocky  
500 Mountains, In: Costa JE, Wicczorek GF (eds) Debris flows/avalanches: process, recognition, and mitigation. Rev Eng Geol  
501 vol. VII. Geol. Soc. Am, doi: <https://doi.org/10.1130/REG7-p115>, 1987.
- 502 Johnsson, A. et al.: Evidence for very recent melt-water and debris flow activity in gullies in a young mid-latitude crater on  
503 Mars, Icarus 235, 37–54, doi: <http://dx.doi.org/10.1016/j.icarus.2014.03.005>, 2014.
- 504 Kirk, R.L., Howington-Kraus, E., Rosiek, M.R., Anderson, J.A., Archinal, B.A., Becker, K.J., Cook, D.A., Galuszka, D.M.,  
505 Geissler, P.E., Hare, T.M., Holmberg, I.M., Keszthelyi, L.P., Redding, B.L., Delamere, W.A., Gallagher, D., Chapel, J.D.,  
506 Eliason, E.M., King, R., McEwen, A.S.: Ultrahigh resolution topographic mapping of Mars with MRO HiRISE stereo images:  
507 meter-scale slopes of candidate Phoenix landing sites, J. Geophys. Res. Planets 113, doi:  
508 <https://doi.org/10.1029/2007JE003000>, 2008.



- 509 Kostaschuk, R.A., Macdonald, G.M., Putnam, P.E.: Depositional process and alluvial fan-drainage basin morphometric  
510 relationships near banff, Alberta, Canada, *Earth Surf. Proc. Land.* 11 (5), 471–484, doi:  
511 <https://doi.org/10.1002/esp.3290110502>, 1986.
- 512 Kreslavsky, M.A.: Slope steepness of channels and aprons: Implications for origin of martian gullies. Workshop Martian  
513 Gullies, Workshop on Martian Gullies 2008. Abs.#1301, 2008.
- 514 Kreslavsky, M.A., Head, J.W.: Mars: nature and evolution of young latitudedependent water-ice-rich mantle, *Geophys. Res.*  
515 *Lett.* 29, doi: <https://doi.org/10.1029/2002GL015392>, 2002.
- 516 Langbein, W. B.: Profiles of rivers of uniform discharge, *U.S. Geol. Surv. Prof. Pap.*, 501-B, 119– 122, doi:  
517 <https://doi.org/10.1086/627653>, 1964.
- 518 Lanza, N. L., Meyer, G. A., Okubo, C. H., Newsom, H. E., & Wiens, R. C.: Evidence for debris flow gully formation initiated  
519 by shallow subsurface water on Mars, *Icarus*, 205(1), 103-112, doi: <https://doi.org/10.1016/j.icarus.2009.04.014>, 2010.
- 520 Levy, J.S. et al.: Identification of gully debris flow deposits in Protonilus Mensae, Mars: Characterization of a water-bearing,  
521 energetic gully-forming process, *Earth Planet. Sci. Lett. Mars Express after 6 Years in Orbit: Mars Geology from Three-*  
522 *Dimensional Mapping by the High Resolution Stereo Camera (HRSC) Experiment 294*, 368–377, doi:  
523 <https://doi.org/10.1016/j.epsl.2009.08.002>, 2010b.
- 524 Levy, J.S., Head, J., Marchant, D.: Thermal contraction crack polygons on Mars: classification, distribution, and climate  
525 implications from HiRISE observations, *J. Geophys.Res. Planets* 114, 01007, doi: <https://doi.org/10.1029/2008JE003273>,  
526 2009a.
- 527 Levy, J. S., Head, J. W., Marchant, D. R., Dickson, J. L., & Morgan, G. A.: Geologically recent gully–polygon relationships  
528 on Mars: Insights from the Antarctic Dry Valleys on the roles of permafrost, microclimates, and water sources for surface  
529 flow, *Icarus*, 201(1), 113-126, doi: <https://doi.org/10.1016/j.icarus.2008.12.043>, 2009b.
- 530 Levy, J.S., Head, J.W., Marchant, D.R.: Gullies, polygons and mantles in Martian permafrost environments: cold desert  
531 landforms and sedimentary processes during recent Martian geological history, *Geol. Soc. Lond. Spec. Publ.* 354, 167–182,  
532 doi: <https://doi.org/10.1144/SP354.10>, 2011.
- 533 Malin, M.C., Edgett, K.S.: Evidence for recent groundwater seepage and surface runoff on Mars. *Science* 288:2330–2335, doi:  
534 <https://doi.org/10.1126/science.288.5475.2330>, 2000.
- 535 Mcewen, A.S., Eliason, E.M. et al.: Mars reconnaissance orbiter’s High Resolution Imaging Science Experiment (HiRISE), *J.*  
536 *Geophys. Res.: Planets*, 112, E05S02, doi: <https://doi.org/10.1029/2005JE002605>, 2007.



- 537 Melton, M.A.: An analysis of the relation among elements of climate, surface properties and geomorphology, Office of Nav.  
538 Res. Dept. Geol. Columbia Univ, NY. Tech. Rep. 11, 1975.
- 539 Milliken, R.E., Mustard, J.F., Goldsby, D.L.: Viscous flow features on the surface of Mars: observations from high-resolution  
540 Mars Orbiter Camera (MOC) images, *J. Geophys. Res.* 108, doi: <https://doi.org/10.1029/2002JE002005>, 2003.
- 541 Mustard, J.F., Cooper, C.D., Rifkin, M.K.: Evidence for recent climate change on Mars from the identification of youthful  
542 near-surface ground ice, *Nature* 412:411–414, doi: <https://doi.org/10.1038/35086515>, 2001.
- 543 Phillips, J.D., Lutz, J.D.: Profile convexities in bedrock and alluvial streams, *Geomorphology* 102, 554–566, doi:  
544 <https://doi.org/10.1016/j.geomorph.2008.05.042>, 2008.
- 545 Pilonget, C. & Forget: Formation of gullies on mars by debris flows triggered by CO<sub>2</sub> sublimation, *Nature Geoscience*, 9, 65–  
546 69, doi: <https://doi.org/10.1038/ngeo2619>, 2016.
- 547 Reiss, D. et al.: Absolute dune ages and implications for the time of formation of gullies in Nirgal Vallis, Mars. *J. Geophys.*  
548 *Res.-Planets* 109, doi: <http://dx.doi.org/10.1029/2004JE002251>, 2004.
- 549 Reiss, D., Hauber, E. et al.: Terrestrial gullies and debris-flow tracks on Svalbard as planetary analogs for Mars, In: Garry,  
550 W.B. & Bleacher, J.E. (eds) *Analogues for Planetary Exploration*, *Geol. Soc. Am. Spec. Papers* 483, 165–175, doi:  
551 [https://doi.org/10.1130/2011.2483\(11\)](https://doi.org/10.1130/2011.2483(11)), 2011.
- 552 Rodine, J.D., Johnson, A.M.: The ability of debris, heavily freighted with coarse clastic materials, to flow on gentle slopes,  
553 *Sedimentology* 23, 213–234, doi: <https://doi.org/10.1111/j.1365-3091.1976.tb00047.x>, 1976.
- 554 Ryder, J.: Some aspects of the morphometry of paraglacial alluvial fans in South-central British Columbia, *Canadian Journal*  
555 *of Earth Sciences* 8: 1252-1264, doi: <https://doi.org/10.1139/e71-11>, 1971.
- 556 Schon, S.C., Head, J.W., Fassett, C.I.: Unique chronostratigraphic marker in depositional fan stratigraphy on Mars: Evidence  
557 for ca. 1.25 Ma gully activity and surficial meltwater origin, *Geology* 37, 207–210, doi: <http://dx.doi.org/10.1130/g25398a.1>,  
558 2009.
- 559 Siewert, M. B., Krautblatter, M., Christiansen, H. H., & Eckerstorfer, M.: Arctic rockwall retreat rates estimated using  
560 laboratory-calibrated ERT measurements of talus cones in Longyeardalen, Svalbard, *Earth Surface Processes and Landforms*,  
561 37(14), 1542-1555, doi: <https://doi.org/10.1002/esp.3297>, 2012.
- 562 Sinha, R. K., Ray, D., De Haas, T., & Conway, S. J.: Global documentation of overlapping lobate deposits in Martian gullies.  
563 *Icarus*, 352, 113979, doi: <https://doi.org/10.1016/j.icarus.2020.113979>, 2020.
- 564 Sinha, R. K., Vijayan, S., Shukla, A. D., Das, P., & Bhattacharya, F.: Gullies and debris-flows in Ladakh Himalaya, India: a  
565 potential Martian analogue, *Geol. Soc. Lond. Spec. Publ.* 467, 315-342, doi: <https://doi.org/10.1144/SP46>, 2019.



- 566 Sinha, R.K., Vijayan, S.: Geomorphic investigation of craters in Alba Mons, Mars: implications for Late Amazonian glacial  
567 activity in the region, *Planet. Space Sci.* 144:32–48, doi: <https://doi.org/10.1016/j.pss.2017.05.014>, 2017.
- 568 Souness, C., & Hubbard, B.: Mid-latitude glaciation on Mars, *Progress in Physical Geography*, 36(2), 238-261, doi:  
569 <https://doi.org/10.1177/030913331243>, 2012.
- 570 Souness, C., Hubbard, B., Milliken, R. E., & Quincey, D.: An inventory and population-scale analysis of martian glacier-like  
571 forms, *Icarus*, 217(1), 243-255, doi: <https://doi.org/10.1016/j.icarus.2011.10.020>, 2012.
- 572 Stock, J.D., Dietrich, W.E.: Erosion of steepland valleys by debris flow, *Geol. Soc. Am. Bull.* 118 (9/10), 1125–1148.  
573 doi:10.1130/B25902.1, 2006.
- 574 Stolle, A., Langer, M., Blöthe, J. H., & Korup, O.: On predicting debris flows in arid mountain belts, *Global and Planetary  
575 Change*, 126, 1-13, doi: <https://doi.org/10.1016/j.gloplacha.2014.12.005>, 2015.
- 576 Welsh, A., Davies, T.: Identification of alluvial fans susceptible to debris-flow hazards. *Landslides* 8 (2), 183–194, doi:  
577 <https://doi.org/10.1007/s10346-010-0238-4>, 2011.
- 578 Wilford, D. J., Sakals, M. E., Innes, J. L., Sidle, R. C., & Bergerud, W. A.: Recognition of debris flow, debris flood and flood  
579 hazard through watershed morphometrics, *Landslides*, 1(1), 61-66, doi: <https://doi.org/10.1007/s10346-003-0002-0>, 2004.
- 580 Yue, Z., Hu, W., Liu, B., Liu, Y., Sun, X., Zhao, Q. and Di, K.: Quantitative analysis of the morphology of martian gullies and  
581 insights into their formation, *Icarus*, 243, pp.208-221, doi: <https://doi.org/10.1016/j.icarus.2014.08.028>, 2014.
- 582